Aluminum Borate Nanowires from the Pyrolysis of Polyaminoborane Precursors

Van An Du, Titel Jurca, George R. Whittell,* Ian Manners*

Supporting Information

Page S3. **Figure S1:** TGA thermograms of polyaminoboranes **1** and **2** (20 →1000 ^{o}C, 10 ^{o}C/min, N_2).

Figure S2: SEM and TEM images from pyrolysis (2 h, at 1000 °C under flow of N_2) of **2** on Si-wafer.

Page S4. **Figure S3:** XRD pattern of h-BN nanostructures grown from the pyrolysis (2 h, at 1000 °C, N_2) of **2** on Si-wafer.

Figure S4: SEM-EDX analysis of amorphous BN-containing nanostructures from the pyrolysis (2 h, at 1000 °C, N_2) of **2** on Si-wafer.

Page S5. **Figure S5:** SEM image from pyrolysis (2 h, at 1000 °C, N_2) of **1** on stainless steel foil.

Figure S6: SEM image from pyrolysis (2 h, at 1000 °C, N_2) of **1** on nickel foil.

Figure S7: SEM-EDX analysis from pyrolysis (2 h, at 1000 °C, N_2) of **1** stainless-steel foil.

Page S6. **Figure S8:** SEM-EDX analysis from pyrolysis (2 h, at 1000 °C, N_2) of **1** on nickel foil.

Figure S9: SEM-EDX analysis of amorphous B and N-containing nanostructures from pyrolysis (2 h, at 1000 °C, N_2) of **1** on rhodium foil.

Figure S10: SEM-EDX analysis of spherical B and N-containing nanostructures from the pyrolysis (2 h, at 1000 °C, N_2) of $H_3N{\cdot}BH_3$ on rhodium foil.

Page S7. **Figure S10:** TEM-EDX analysis of Al_5BO_9 nanowires grown by pyrolysis (2 h, at 1000 °C, N_2) of **1** on sapphire with defects.

Figure S12: WDS analysis of Al_5BO_9 nanowires grown by pyrolysis (2 h, at 1000 °C under flow of N_2) of **1** on sapphire with defects.

Page S8. **Figure S13:** XRD pattern of Al_5BO_9 nanowires grown from the pyrolysis (2 h, at 1000 °C, N_2) of a (1:1 by mass) mixture of Al_2O_3 powder and **1**.

Figure S14: HRTEM image of Al_5BO_9 nanowires grown from the pyrolysis (2 h, at 1000 °C under flow of N_2) of a (1:1 by mass) mixture of Al_2O_3 powder and **1**.

Page S9. **Figure S15:** SEM-EDX analysis of Al_5BO_9 nanowires grown from pyrolysis (2 h, at 1000 °C, N_2) of a (1:1 by mass) mixture of Al_2O_3 powder and **1**.

Figure S16: WDS analysis of Al_5BO_9 nanowires grown from the pyrolysis (2 h, at 1000 °C under flow of N_2) of a (1:1 by mass) mixture of Al_2O_3 powder and **1**.

Figure S17: TEM-EDX analysis of the amorphous coating (see Figure 5c) of the Al_5BO_9 nanowires grown from the pyrolysis (2 h, at 1000 °C under flow of N_2) of a (1:1 by mass) mixture of Al_2O_3 powder and **1**.

Page S10. **Figure S18:** XRD pattern of Al_5BO_9 nanowires grown from the pyrolysis (2 h, at 1000 °C, N_2) of a (1:1 by mass) mixture of AlN powder and **1**.

Figure S19: SEM-EDX measurement of Al_5BO_9 nanowires grown from the pyrolysis (2 h, at 1000 °C, N_2) of a (1:1 by mass) mixture of AlN powder and **1**.

Page S11. **Figure S20:** WDS measurements of Al_5BO_9 nanowires grown from the pyrolysis (2 h, at 1000 °C, N_2) of a (1:1 by mass) mixture of AlN powder and **1**.

Figure S21: SEM image from pyrolysis (2 h, at 1300 °C, N_2) of **2** on annealed sapphire wafer.

Page S12. **Figure S22:** XRD pattern of Al_5BO_9 nanowires grown from the pyrolysis (2 h, at 1300 °C, N_2) of **2** on annealed sapphire wafer.

Figure S23: SEM-EDX analysis of Al_5BO_9 nanowires grown from the pyrolysis (2 h, at 1300 °C, N_2) of **2** on annealed sapphire wafer.

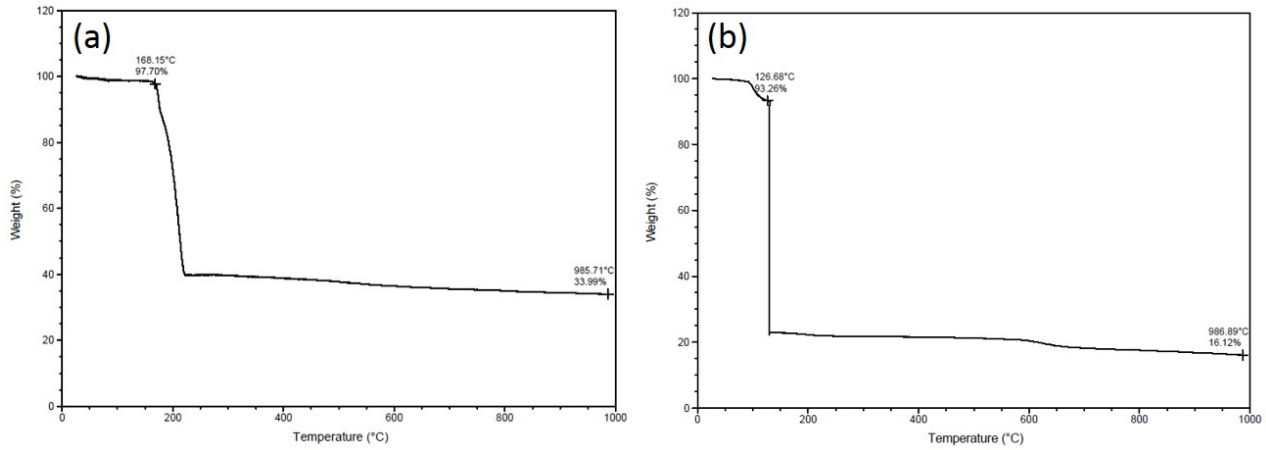

Figure S1: TGA thermograms of polyaminoboranes **1** (a) and **2** (b) from 20 to 1000 ^{o}C with a heating rate of 10 ^{o}C/min under flow of N_2.

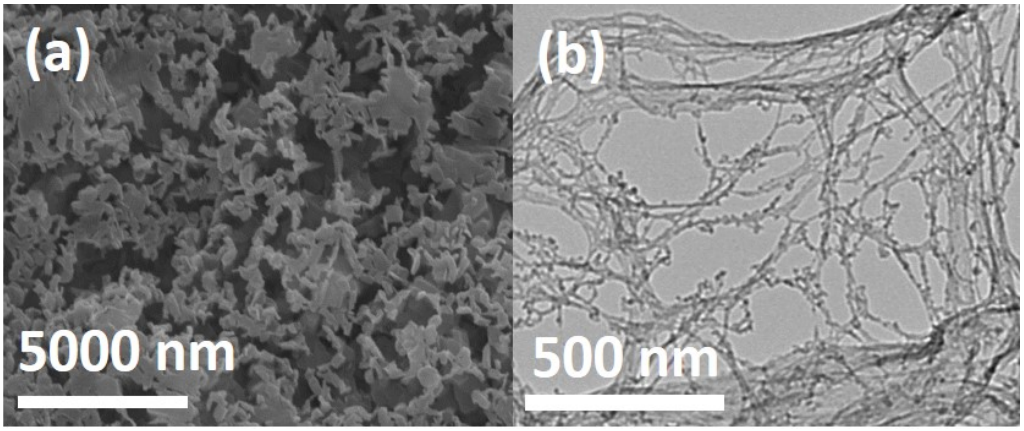

Figure S2: Electron microscopy images of BN-containing micro- and nano-scale structures grown from the pyrolysis (2 h, at 1000 °C under flow of N_2) of polyaminoborane **2** on a Si-wafer: (a) SEM image, (b) TEM image.

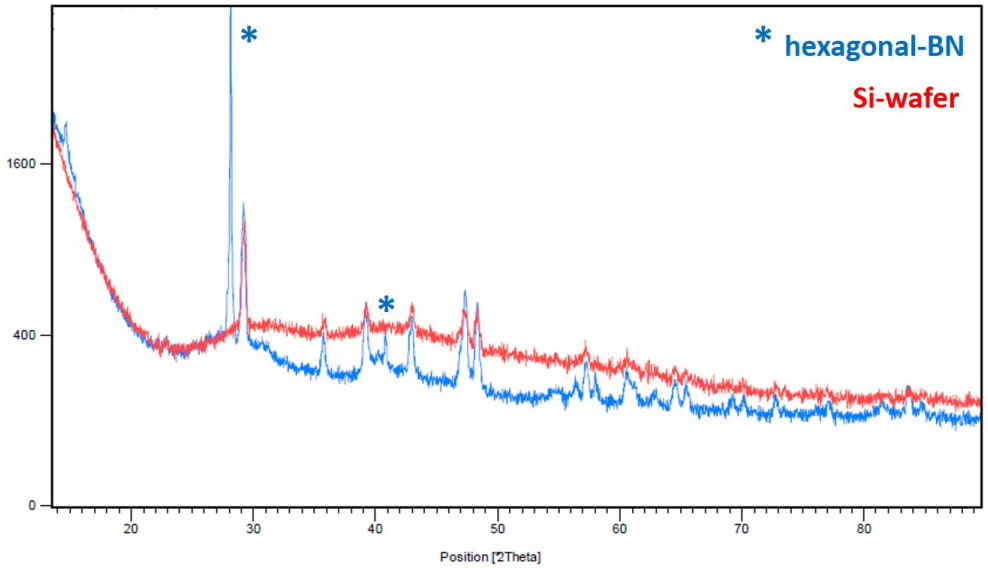

Figure S3: XRD analysis of h-BN structures grown from the pyrolysis (2 h, at 1000 °C under flow of N_2) of **2** on Si-wafer (blue), compared to blank Si-wafer (red). The two peaks at 2θ = 27.8 and 2θ = 40.9° were indexed to the (0 0 2) and (1 0 0) lattice planes of h-BN (ICSD: 168892).

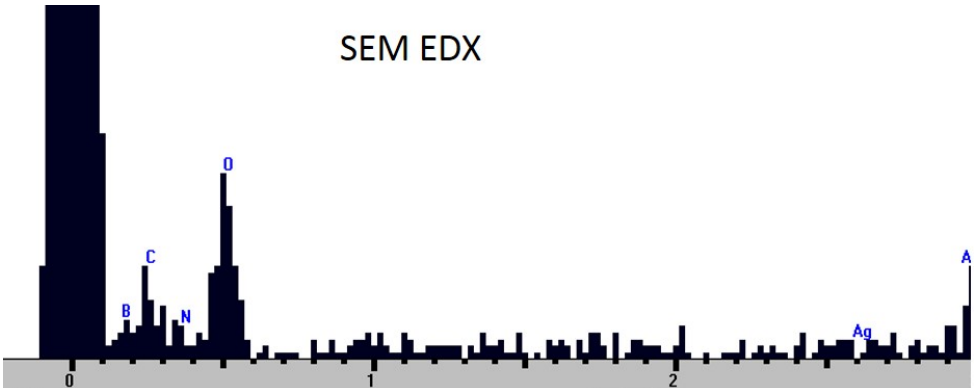

Figure S4: SEM-EDX analysis of amorphous BN-containing nanostructures grown from the pyrolysis (2 h, at 1000 °C under flow of N_2) of **2** on Si-wafer.

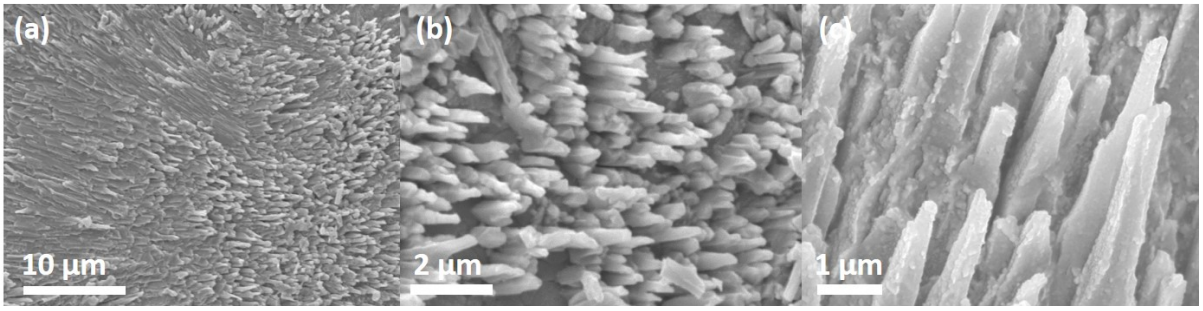

Figure S5: (a-c) SEM images from pyrolysis (2 h, at 1000 °C under flow of N_2) of **1** on stainless steel foil (composition Fe:Cr:Ni; 70:19:11 wt%).

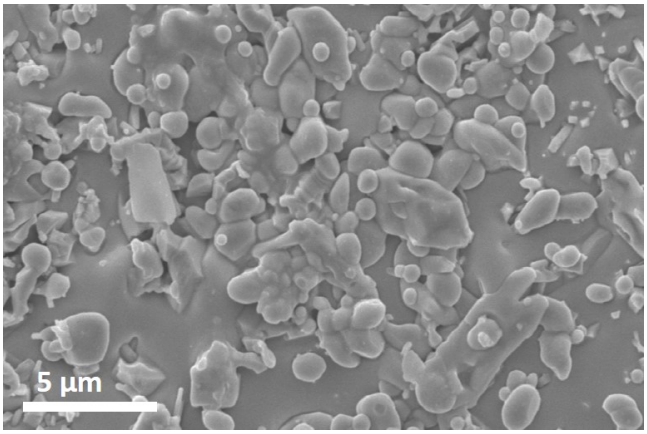

Figure S6: SEM image from pyrolysis (2 h, at 1000 °C under flow of N_2) of **1** on nickel foil (99%).

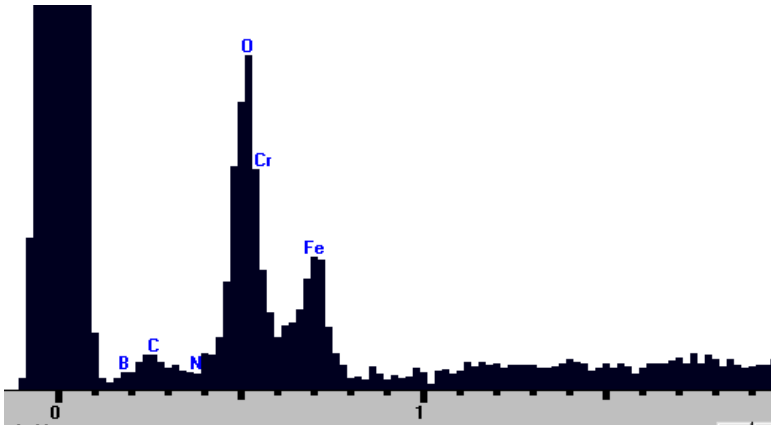

Figure S7: SEM-EDX analysis of the product from pyrolysis (2 h, at 1000 °C under flow of N_2) of **1** on stainless-steel foil (composition Fe:Cr:Ni; 70:19:11 wt%).

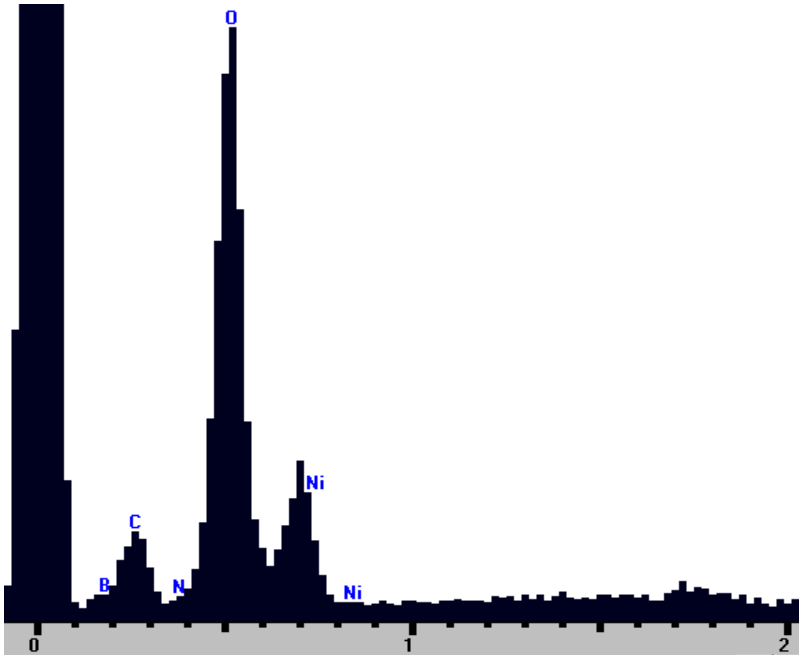

Figure S8: SEM-EDX analysis of the product from pyrolysis (2 h, at 1000 °C under flow of N_2) of **1** on nickel foil (99%).

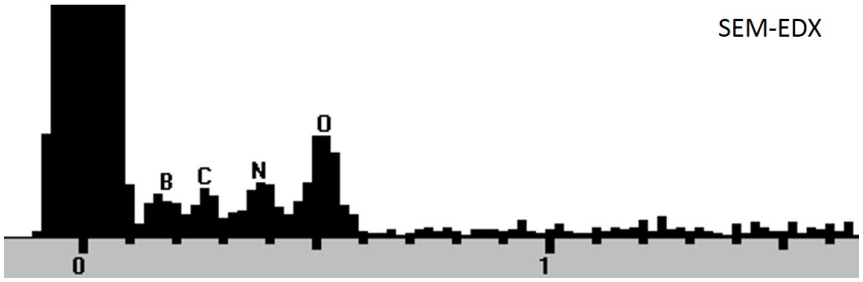

Figure S9: SEM-EDX analysis of amorphous B and N-containing nanostructures grown from pyrolysis (2 h, at 1000 °C under flow of N_2) of **1** on rhodium foil.

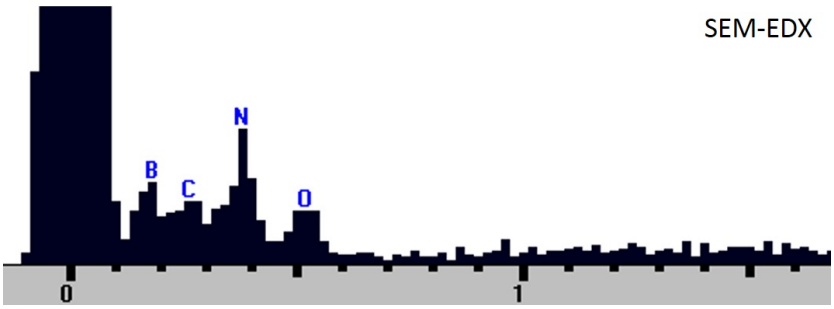

Figure S10: SEM-EDX analysis of spherical B and N-containing nanostructures grown from the pyrolysis (2 h, at 1000 °C under flow of N_2) of $H_3N{\cdot}BH_3$ on rhodium foil.

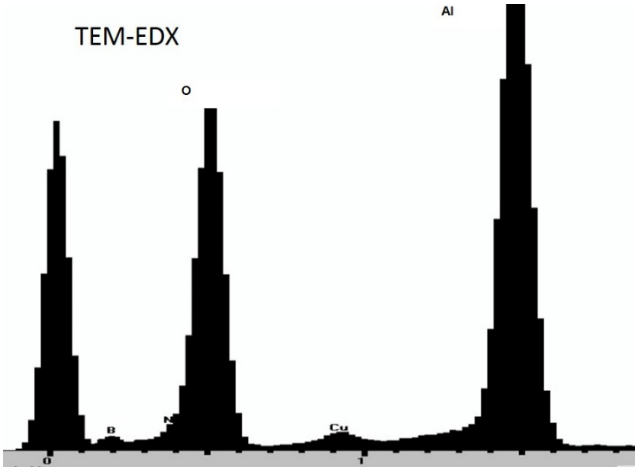

Figure S11: TEM-EDX analysis of Al_5BO_9 nanowires grown by pyrolysis (2 h, at 1000 °C under flow of N_2) of **1** on sapphire with defects.

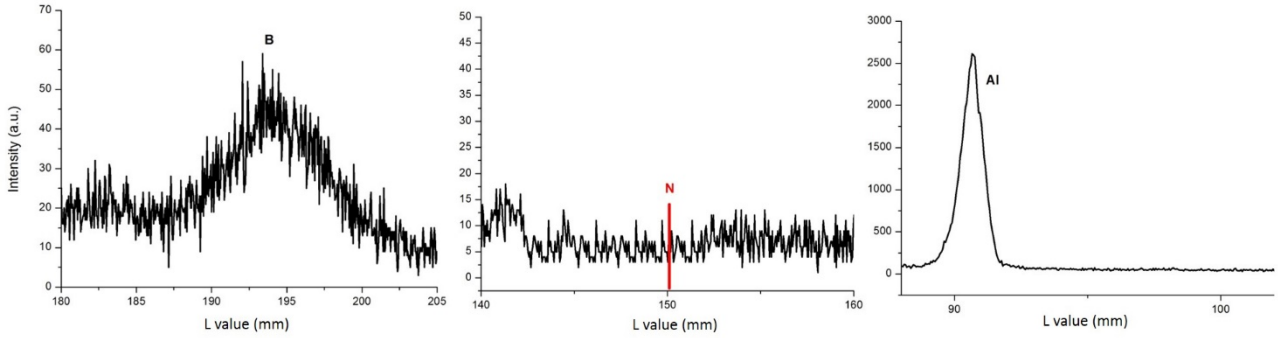

Figure S12: WDS analysis of Al_5BO_9 nanowires grown by pyrolysis (2 h, at 1000 °C under flow of N_2) of **1** on sapphire with defects. (*left*: B; *middle*: shows lack of N; *right*: Al)

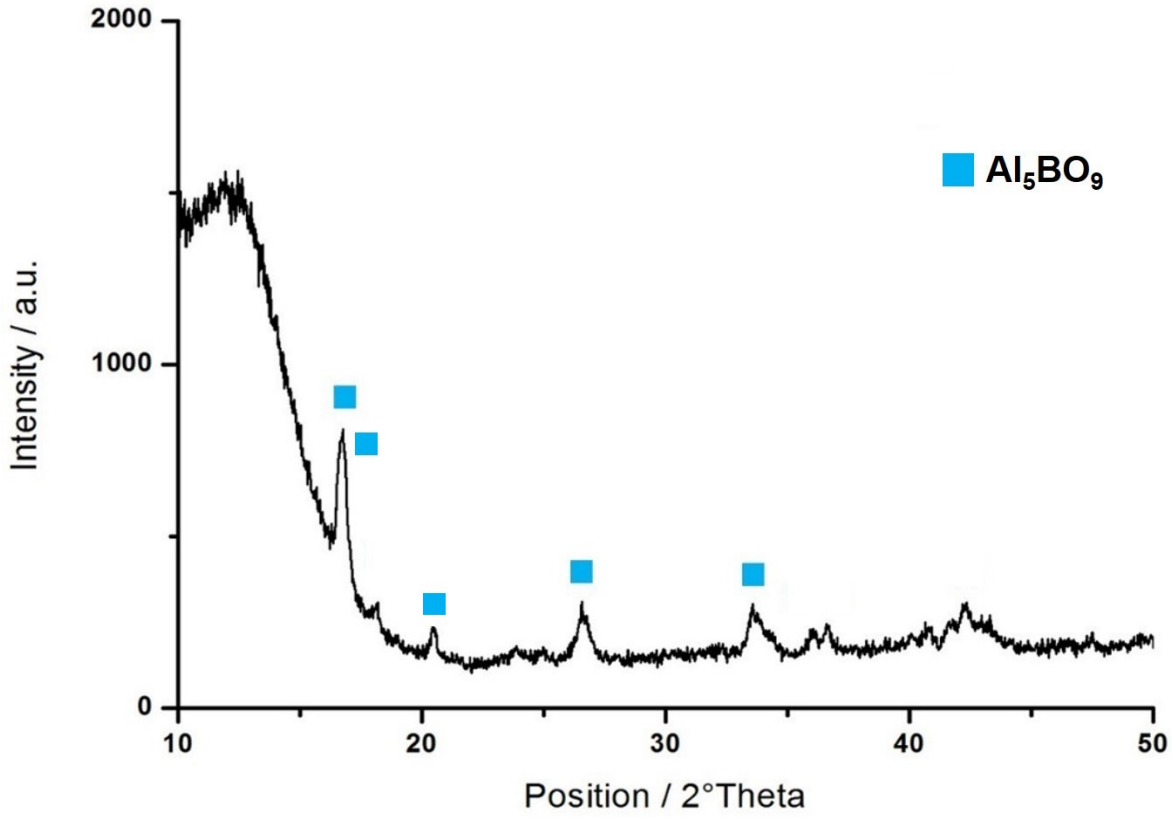

Figure S13: XRD pattern of Al_5BO_9 nanowires grown from the pyrolysis (2 h, at 1000 °C under flow of N_2) of a (1:1 by mass) mixture of Al_2O_3 powder and **1**. The peaks at 2θ = 16.7, 17.0, 20.4, 26.7 and 33.7° were indexed to the (0 2 1), (1 1 0), (1 1 1), (1 3 1) and (1 3 2) planes of the orthorhombic phase of Al_5BO_9 (ICSD: 039013).

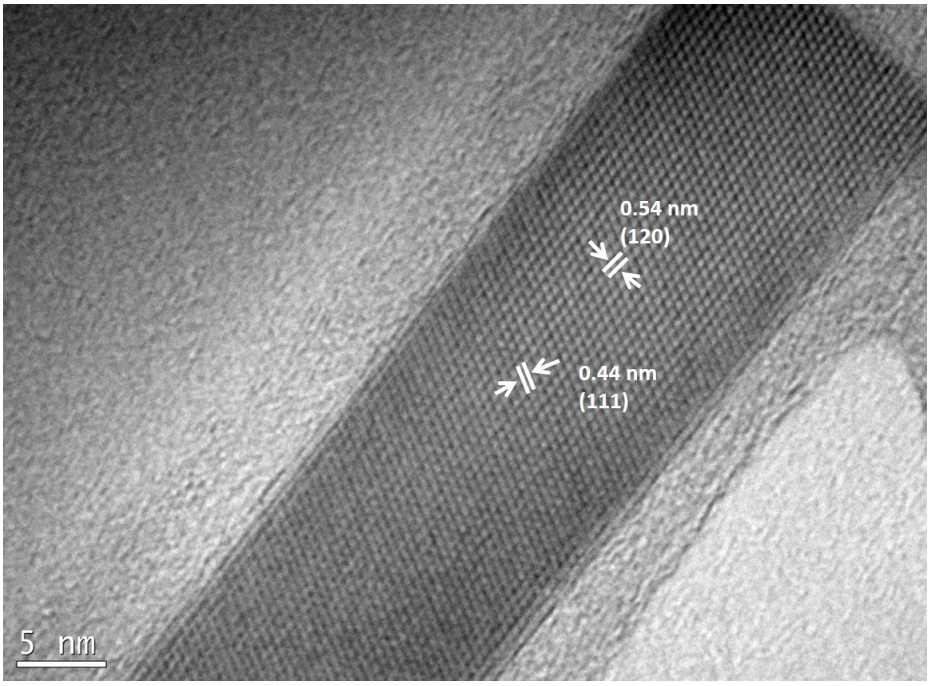

Figure S14: High resolution transmission electron microscope image of Al_5BO_9 nanowires grown from the pyrolysis (2 h, at 1000 °C under flow of N_2) of a (1:1 by mass) mixture of Al_2O_3 powder and **1**. The lattice fringes reveal d-spacings of 0.44 nm and 0.54 nm, which were indexed to the (1 1 1) and (1 2 0) planes of Al_5BO_9 (ICSD: 039013), respectively.

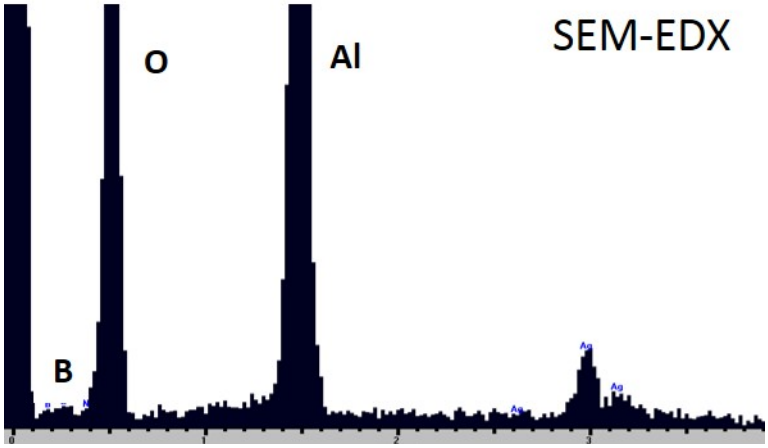

Figure S15: SEM-EDX analysis of Al_5BO_9 nanowires grown from the pyrolysis (2 h, at 1000 °C under flow of N_2) of a (1:1 by mass) mixture of Al_2O_3 powder and **1**.

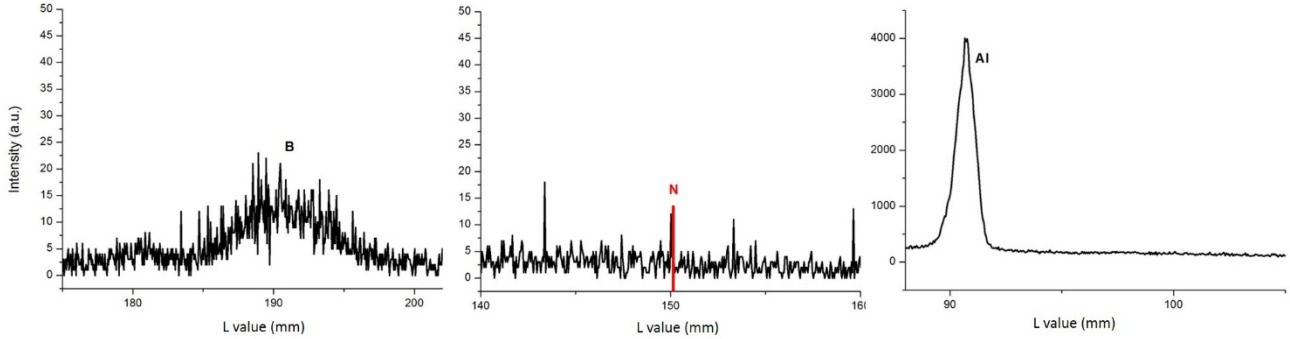

Figure S16: WDS analysis of Al_5BO_9 nanowires grown from the pyrolysis (2 h, at 1000 °C under flow of N_2) of a (1:1 by mass) mixture of Al_2O_3 powder and **1**. (*left*: B; *middle*: shows lack of N; *right*: Al)

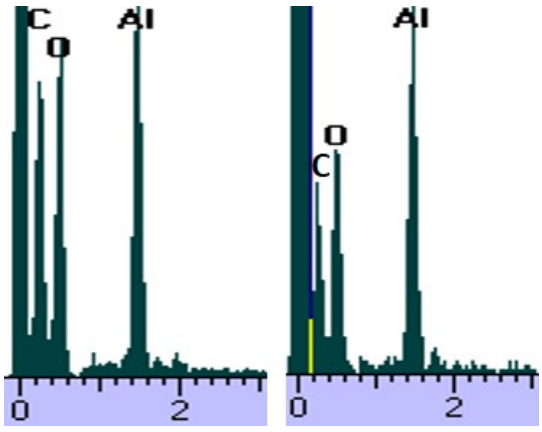

Figure S17: TEM-EDX analysis (two spots measured on same sample) focusing mainly on the coating (see Figure 5c) of the Al_5BO_9 nanowires grown from the pyrolysis (2 h, at 1000 °C under flow of N_2) of a (1:1 by mass) mixture of Al_2O_3 powder and **1**.

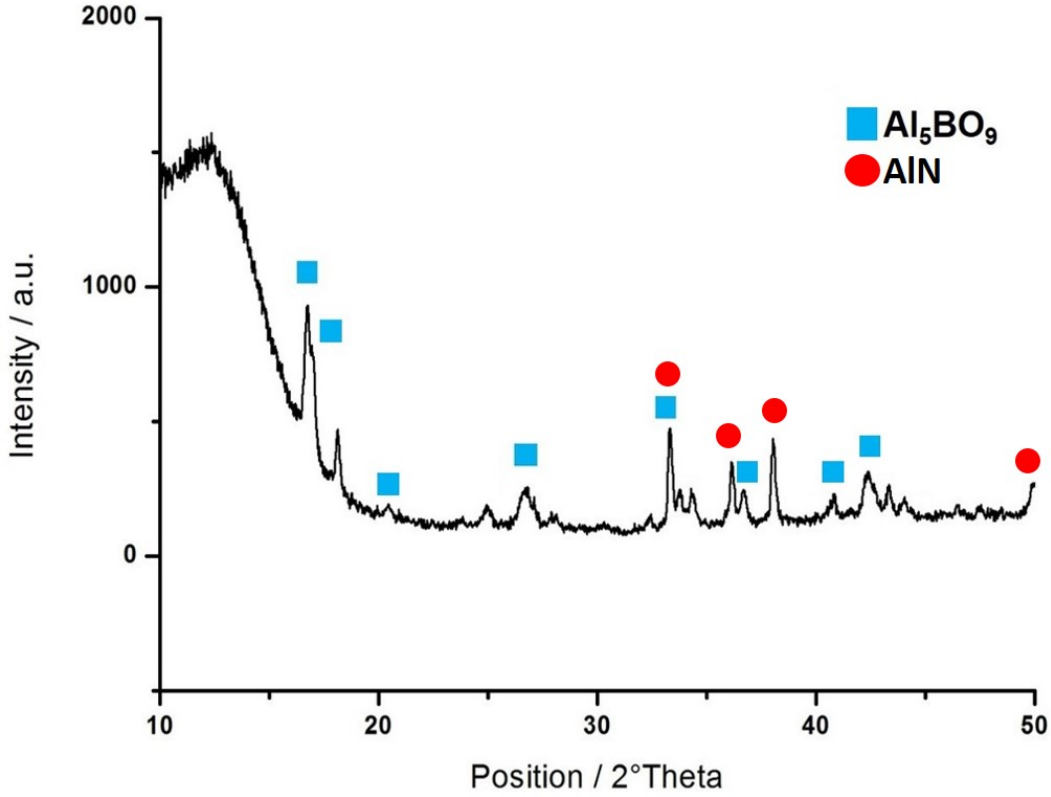

Figure S18: XRD analysis of Al_5BO_9 nanowires grown from the pyrolysis (2 h, at 1000 °C under flow of N_2) of a (1:1 by mass) mixture of AlN powder and **1**. The peaks at 2θ = 16.7, 17.0, 20.4, 26.7 and 33.7° were indexed to the (0 2 1), (1 1 0), (1 1 1), (1 3 1) and (1 3 2) planes of the orthorhombic phase of Al_5BO_9 (ICSD: 039013).

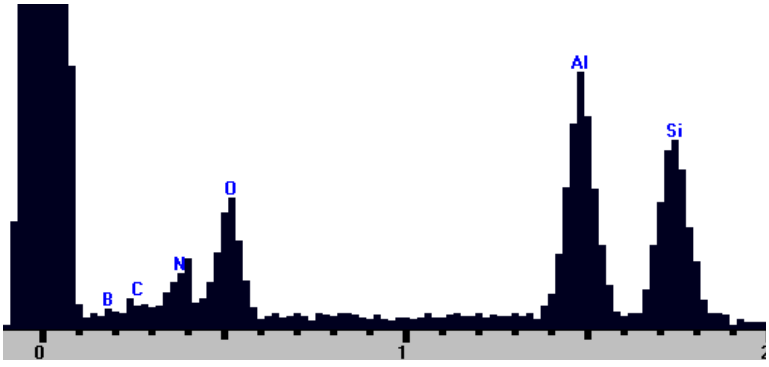

Figure S19: SEM-EDX analysis of Al_5BO_9 nanowires grown from the pyrolysis (2 h, at 1000 °C under flow of N_2) of a (1:1 by mass) mixture of AlN powder and **1**.

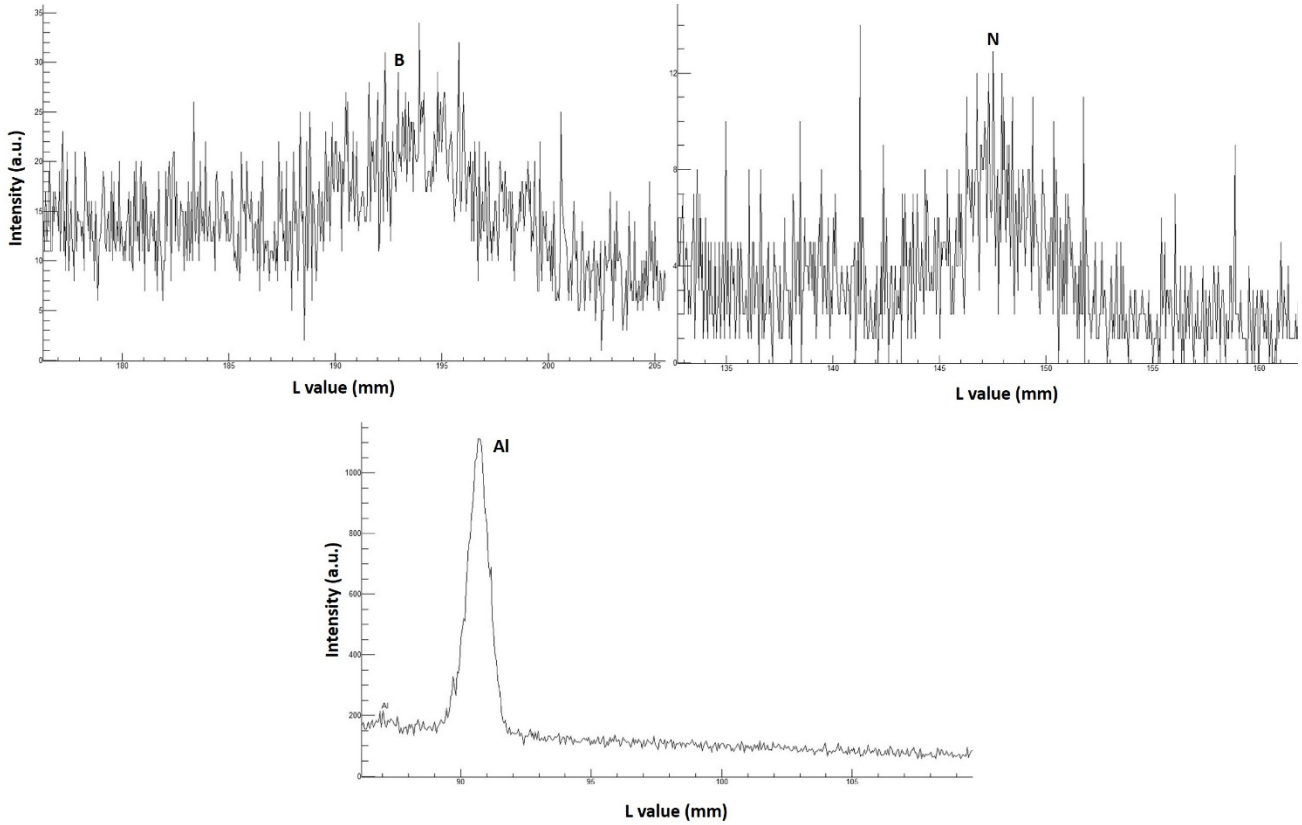

Figure S20: WDS analysis of Al_5BO_9 nanowires grown from the pyrolysis (2 h, at 1000 °C under flow of N_2) of a (1:1 by mass) mixture of AlN powder and **1**. (*left*: B; *middle*: N; *right*: Al).

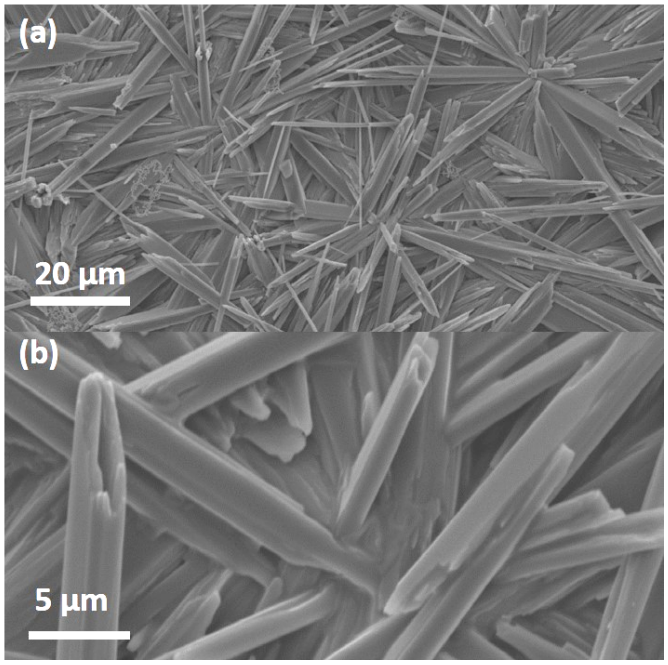

Figure S21: SEM images from Al_5BO_9 nanostructures grown from the pyrolysis (2 h, at 1300 °C under flow of N_2) of **2** on annealed sapphire wafer.

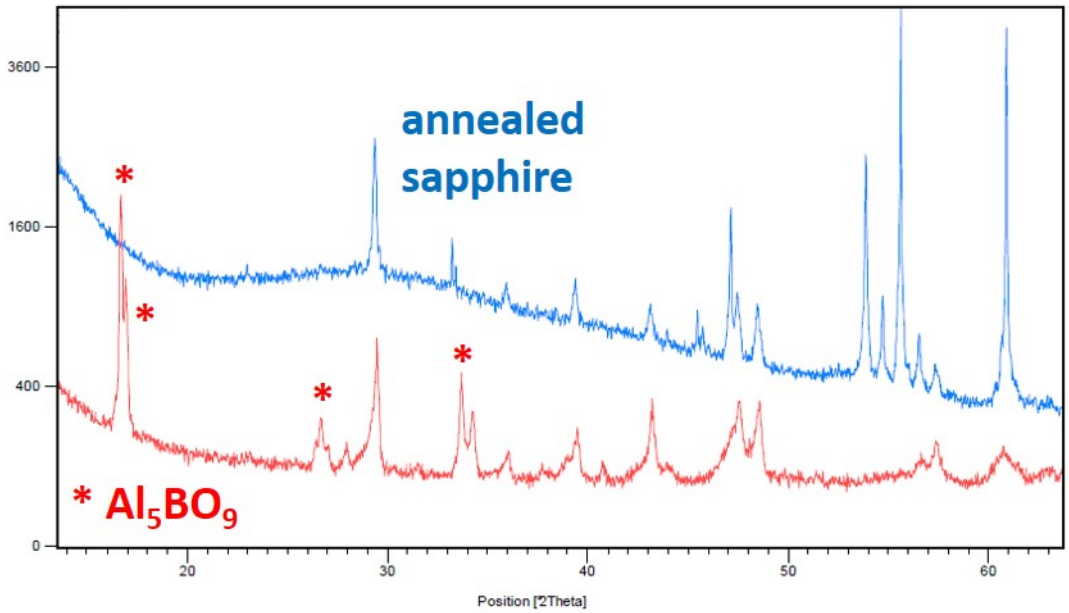

Figure S22: XRD pattern of Al_5BO_9 nanowires grown from the pyrolysis (2 h, at 1300 °C under flow of N_2) of **2** on annealed sapphire wafer (red), compared to blank annealed sapphire wafer (blue). The peaks at 2θ = 16.7, 17.0, 26.7 and 33.7° were indexed to the (0 2 1), (1 1 0), (1 3 1) and (1 3 2) planes of the orthorhombic phase of Al_5BO_9 (ICSD: 039013).

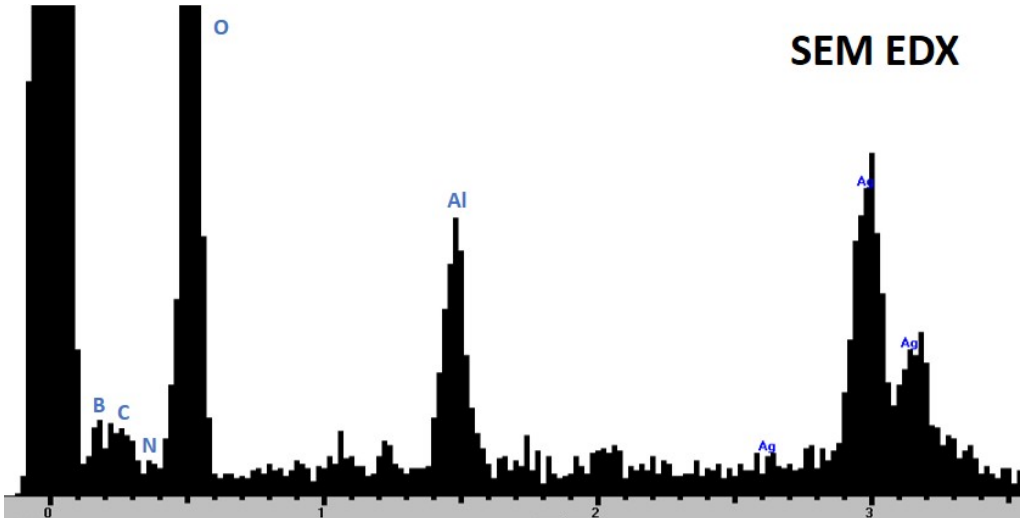

Figure S23: SEM-EDX analysis of Al_5BO_9 nanowires grown from the pyrolysis (2 h, at 1300 °C under flow of N_2) of **2** on annealed sapphire wafer.